Computer Methods and Programs in Biomedicine 144 (2017) 135–145

Contents lists available at ScienceDirect

Computer Methods and Programs in Biomedicine

journal homepage: www.elsevier.com/locate/cmpb

A novel method for planning liver resections using deformable Bézier surfaces and distance maps

Rafael Palomar[a,b,*], Faouzi A. Cheikh[a], Bjørn Edwin[b,e,f], Åsmund Fretland[b,e,f], Azeddine Beghdadi[c], Ole J. Elle[b,d]

[a] Department of Computer Science, NTNU, 2815 Gjøvik, Norway
[b] The Intervention Centre, Oslo University Hospital, P.O. box 4950 - Nydalen, 0424 Oslo, Norway
[c] L2TI, Institut Galilée, Université Paris 13, Avenue J. B. Clément 99, 93430 Villetaneuse, France
[d] Department of Informatics, University of Oslo, 0373 Oslo, Norway
[e] Department of Hepato-Pancreato-Biliary Surgery, Oslo University Hospital, P.O. box 4950 - Nydalen, 0424 Oslo, Norway
[f] Institute of Clinical Medicine, University of Oslo, Norway

ARTICLE INFO

Article history:
Received 1 July 2016
Revised 22 February 2017
Accepted 21 March 2017

Keywords:
Liver resection
Bézier surfaces
Distance maps
Surgery planning
Visualization

ABSTRACT

Background and Objective: For more than a decade, computer-assisted surgical systems have been helping surgeons to plan liver resections. The most widespread strategies to plan liver resections are: drawing traces in individual 2D slices, and using a 3D deformable plane. In this work, we propose a novel method which requires low level of user interaction while keeping high flexibility to specify resections. *Methods:* Our method is based on the use of Bézier surfaces, which can be deformed using a grid of control points, and distance maps as a base to compute and visualize resection margins (indicators of safety) in real-time. Projection of resections in 2D slices, as well as computation of resection volume statistics are also detailed. *Results:* The method was evaluated and compared with *state-of-the-art* methods by a group of surgeons ($n = 5$, 5–31 years of experience). Our results show that theproposed method presents planning times as low as *state-of-the-art* methods (174 *s* median time) with high reproducibility of results in terms of resected volume. In addition, our method not only leads to smooth virtual resections easier to perform surgically compared to other *state-of-the-art* methods, but also shows superior preservation of resection margins. *Conclusions:* Our method provides clinicians with a robust and easy-to-use method for planning liver resections with high reproducibility, smoothness of resection and preservation of resection margin. Our results indicate the ability of the method to represent any type of resection and being integrated in real clinical work-flows.

1. Introduction

Liver cancer is one of the most common causes of cancer death worldwide and its frequency is increasing in some geographical areas of historically low incidence rates [1]. Liver resection, which refers to the surgical removal of a liver tumor, is the only curative treatment for liver cancer. Planning of liver resections is usually based on the anatomic division of the liver in segments, as described in Couinaud [2]. The Couinaud division, which presents a wide consensus in the medical community, separates the liver into 8 areas (segments) according to the blood supply, and establishes a framework for the classification of resections in different types [3].

Liver cancer is either primary (arising from normal liver tissue) or secondary (spreading to the liver from cancer located in other organs). For hepatocellular carcinoma (primary), which accounts for 70%-80% of the liver cancer cases worldwide [4], surgical resection is the treatment of choice and is considered to be potentially curative [5]. Selected patients with metastatic (secondary) liver tumors—which develop in 50% of the cases of colorectal cancer—present up to 58% increased 5-year survival rates after liver resection [6].

In contemporary liver surgery, pre-operative planning becomes increasingly important. New techniques like parenchymal-sparing [7] can use pre-operative planning to help surgeons optimizing the resection path, potentially increasing the remnant liver. Volume expanding techniques (like associating liver partition and portal split (ALPPS) [8], and portal vein embolization) can also

* Corresponding author:
E-mail address: rafael.palomar@ntnu.no (R. Palomar).

http://dx.doi.org/10.1016/j.cmpb.2017.03.019

make use of pre-operative planning to derive the volumetry of the resection. This can help ensuring that remnant liver is large enough and with sufficient function to prevent post-operative liver failure.

For nearly two decades, surgeons and other clinicians have employed computer-assisted surgical systems to support the decision-making process for planning and guiding surgical interventions. In the case of liver resections, these systems have recently been evaluated in the clinical practice and have shown improvements not only in tumor localization and precision of surgery planning [9–11], but also an improved orientation and confidence of the surgeon during the operation [12].

Liver resection planning systems are based on the definition of *virtual resections* [13]. Virtual resections help clinicians to visualize the resection (surgical cutting path), affected vessels and resection margins (safety distance kept between the tumors and the resection path). In addition, virtual resections allow the computation of the estimated resected volume.

Simplicity of use and flexibility to specify the virtual resections are key features of surgery planning systems. Simplicity and flexibility are often considered as diverging objectives—simple interactions usually impose constraints on the freedom to describe virtual resections. The two most common strategies proposed for specification of virtual resections are: drawing traces in 2D individual slices [14] (**DS**) and definition of and virtual resections defined using a deformable cutting plane [15] (**CP**).

1.1. Contribution

In this work, we present a new method for planning liver resection procedures. The novelty of our method is twofold. On one hand, our method is based on the use of Bézier surfaces, which can be deformed in real-time solely by a set of control points. On the other hand, we propose the use of distance maps to project the safety margins in real-time onto the resection surface, thus allowing the user to modify the resection proposal until the safety requirements are met.

In addition, an implementation of the method based on the open-source software *3D Slicer* [16] is presented. This implementation includes interaction mechanisms which not only avoid the use of manual drawing of lines (both in the 3D model as in CP, and in the 2D slices as in DS), but also presents a flexible yet simple way to define virtual resections regardless of their type (e.g., hemihepatectomy, parenchymal-sparing). Details on visualization aspects, projection of resection surfaces onto individual 2D slices, as well as resected volume computation based on our method, are also detailed.

2. Theoretical background

In this section, we briefly describe the foundations of Bézier tensor product surfaces and some of their most important properties. A deeper description can be found in [17–19]. For simplicity and clarity reasons, in this work we focus on parametric non-rational Bézier surfaces, however, the methods described in this work can be easily adapted to other Bézier formulations.

Formally, a parametric non-rational Bézier surface $\mathbf{S} \in \mathbb{R}^3$ of degree (m, n) can be defined as:

$$\mathbf{S}(u,v) = \sum_{i=0}^{m}\sum_{j=0}^{n} \mathbf{C}_{i,j} B_{i,m}(u) B_{j,n}(v), \tag{1}$$

with $u, v \in [0, 1]$. $\mathbf{C}_{i,j} \in \mathbb{R}^3$ are the control points characterizing the shape of the surface, and the i-th and j-th bases, $B_{i,m}$ and $B_{j,n}$ with degrees m and n respectively, are Bernstein polynomials given by:

$$B_{i,m}(t) = \binom{m}{i}(1-t)^{(m-i)}t^i. \tag{2}$$

Lemma 1. *Let* $\mathbf{S}$ *be a parametric bi-linear Bézier surface of degree* (m, n) *as described in Eq. (1). Such surface, has the following properties:*

(a) *Surface contained in the convex hull* $\mathbb{CH}$*:*

$$\mathbf{S}(u,v) \in \mathbb{CH}(\mathbf{C}_{0,0}, \ldots, \mathbf{C}_{m,n}) \ \forall (u,v). \tag{3}$$

(b) *Affine transformation invariance:*

$$\mathbf{T}(\mathbf{S}) = \sum_{i=0}^{m}\sum_{j=0}^{m} \mathbf{T}(\mathbf{C}_{i,j}) B_{i,p}(u) B_{j,q}(v), \tag{4}$$

where T is an affine transformation (i.e., rotation, reflection, translation or scaling).

(c) *Polyhedral approximation: under triangulation, the net of control points forms a planar polyhedral approximation of the surface.*

A proof for these properties follows easily from the proof of the analogous properties for Bézier curves [17]. In the remaining of the document, we will refer to these properties to justify design aspects and properties of the proposed method.

3. Materials and methods

3.1. Overview of the method

Regardless of the type of model supporting the definition of virtual resections (i.e., voxel-based or 3D models), models employed in planning of liver resection ultimately rely on patient-specific segmented models typically obtained from computed tomography (**CT**).

The approach presented in this work is entirely supported by patient-specific 3D models. In order to construct these models, first, a medical image is obtained from CT. Medical images are represented as scalar fields $F : \mathbb{R}^3 \to \mathbb{R}$ where the points $\{\mathbf{p}_i \in \mathbb{R}^3\}_{i=1}^{N}$ present intensity values $F(\mathbf{p}_i) = v$. Through segmentation, different tissues (i.e., vessels, parenchyma[1] and tumors) are separated in a new scalar field $S : \mathbb{R}^3 \to \{l_1, \ldots, l_k\}$ with k classes (tissues). Finally, through isosurface extraction methods, like marching cubes [20,21], 3D models of the labeled tissues are obtained.

In computer graphics, surface descriptions such as 3D models and Bézier surfaces are commonly represented as triangle meshes. In the remaining of this work, triangular meshes are denoted as sets $\mathcal{M} = \{V, T\}$ with vertices $V = \{0, 1, 2, \ldots\}$ and its associated positions $\mathbf{p}_i \in \mathbb{R}^3$, edges $E = \{(i, j) | i, j \in V\}$, and triangles $T = \{(i, j, k) | (i, j), (j, k), (k, i) \in E\}$.

As in CP approaches, the work-flow of our approach (Fig. 1), consists of two steps: initialization (planar approximation) and modification of the resection. The differences with other CP approaches like [15] lie in the underlying representation, and deformation methods. This not only leads to new properties of the resection surfaces, but also to different user interaction schemes. In our method, first, the 3D mesh models $\mathcal{M}_p$ (parenchyma) and $\mathcal{M}_t$ (tumor) generated previously, are used to define a planar contour around the parenchyma. Unlike in CP, user interaction required to specify the contour is not based on manual drawing, but on a slicing movable plane (Section 3.2). This contour leads to the generation of a planar resection surface. In a second step, the user can deform the planar surface by means of a grid of control points (Section 3.3).

3.2. Initialization of the resection

The goal of this process is to obtain a first approximation (planar Bézier) of the resection surface which will be used as a starting

[1] In this work, the term parenchyma is used to refer to the part of the liver which is neither tumor tissue nor blood vessels.

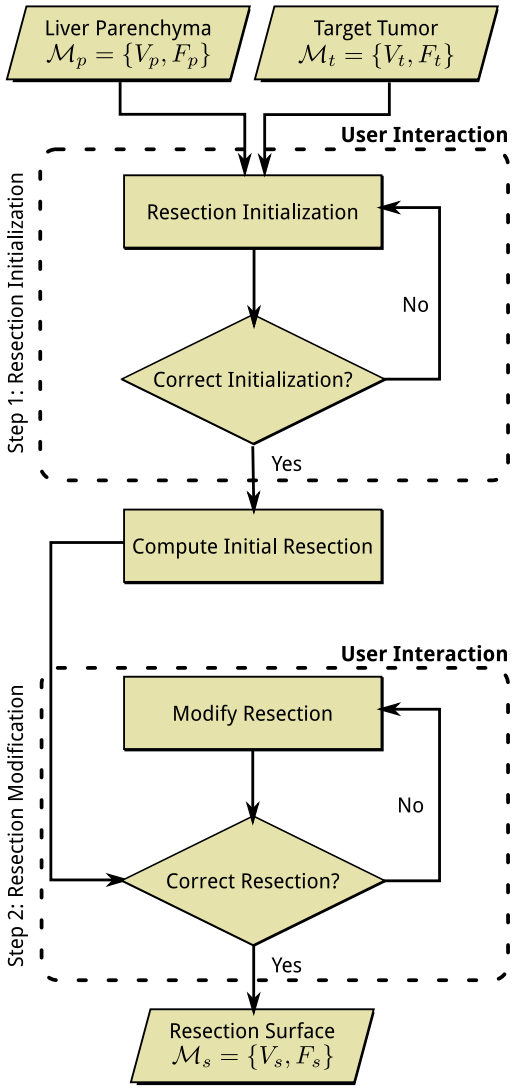

Fig. 1. Flow chart of the proposed method.

point for subsequent modifications. In order to obtain this approximation, the user is first provided with the 3D representation of the liver and tumor, as illustrated in Fig. 2a and 2b. Together with these anatomic representations, a line connecting the centroid of the tumor $\mathbf{c}$ with an arbitrarily placed 3D end-point $\mathbf{p}_e$ (in Fig. 2a, b this corresponds to $\mathbf{p}_{end0}$ and $\mathbf{p}_{end1}$ in different interaction times) is displayed. This line is associated to an invisible plane P (in Fig. 2a this corresponds to P_0 and P_1 at different interaction times) passing through the middle point of the line connecting $\mathbf{c}$ and a end-point $\mathbf{p}_e$ which satisfies the point-normal form:

$$\underbrace{(\mathbf{p}_e - \mathbf{c})}_{\vec{\mathbf{n}}} \cdot \left(\mathbf{x} - \left(\frac{\mathbf{c} + \mathbf{p}_e}{2}\right)\right) = 0. \tag{5}$$

The plane P is then used to slice the parenchyma model $\mathcal{M}_p$, thus providing a contour representation V_s (ring around the parenchyma in Fig. 2b). User interaction takes place by moving the 3D end-point $\mathbf{p}_e$. The effect of moving this end-point is the modification of the slicing plane, which effectively creates a contour (around the parenchyma) moving in real-time. This initialization process is formally described in Algorithm 1.

The resulting contour V_s is then used to compute resection approximation in terms of a planar surface (Fig. 2c). Similarly to [15], the origin, extent and orientation of this plane is obtained

Algorithm 1 Computation of resection contour.

Precondition: User-defined end point $\mathbf{p}_e$ inside parenchyma mesh $\mathcal{M}_p$.

```
1: function CONTOUR(M_p, M_t, p_e )
2:     c ← Centroid(M_t)                    ▷ Centroid of tumor
3:     n ← p_e − c                          ▷ Normal vector
4:     P ← Plane((p_e+c)/2, n)              ▷ Slicing plane P ⊥ n
5:     V_s ← Slice(M_p, P)                  ▷ Point-based contour
6:     return V_s
7: end function
```

by means of principal component analysis (**PCA**). The orientation of the initial resection is given by the two eigenvectors $\vec{\mathbf{E}}_1$ and $\vec{\mathbf{E}}_2$ presenting the larger eigenvalues e_1 and e_2. These eigenvalues, are then used to compute the size of the initial resection, in our case:

$$\begin{cases} l_1 = 4\sqrt{e_1} \\ l_2 = 4\sqrt{e_2} \end{cases}. \tag{6}$$

The election of the lengths l_i is based on the consideration of $\sqrt{e_i}$ as estimators of the standard deviations of the contour V_s along the eigenvectors $\vec{\mathbf{E}}_i$. Assuming uniform distribution of the contour along these eigenvectors, l_i exceeds the length of the contour, and therefore, the initial plane also exceeds the boundaries of the parenchyma.

The origin of the plane (center) is computed with respect to the centroid of the contour V_s. First the centroid is computed using all the points that make up the contour:

$$\mathbf{c} = \frac{1}{N}\sum_{i=1}^{N} \mathbf{p}_i \ , \ \ \mathbf{p}_i \in V_s. \tag{7}$$

Then the origin is computed as the translation of the centroid in the direction $(-\vec{\mathbf{E}}_1, -\vec{\mathbf{E}}_2)$ by half the extent of the plane on each direction, this is:

$$\mathbf{o} = \mathbf{c} - \frac{l_1}{2}\vec{\mathbf{E}}_1 - \frac{l_2}{2}\vec{\mathbf{E}}_2. \tag{8}$$

Once the geometry of the initial resection is computed, we map a 2D grid of $m \times n$ equally spaced points. This grid of points will serve as a base to build a deformable Bézier surface—from Lemma 1.a it follows that, if all control points lie in a plane, the associated Bézier surface also lies on the same plane. Formally, this process is described in Algorithm 2.

3.3. Deformation of Bézier surfaces

Deformation of a Bézier tensor-product surface is performed through the interactive manipulation of the coordinates of the control points (distributed in a connected grid). The control points do not normally lie on the surface (except for the corners, which always lie in the surface). The fact that the net of control points is an approximation of the surface (Lemma 1.c) makes that the deformations of the surface occur in coherence with the manipulation of the control points.

The number of control points is an important design consideration. On one hand, increasing the number of control points increases the number of interactions as the user may have to modify more control points. On the other hand, and as derived from Eqs. (1) and (2), the number of control points determines the degree of the surface, and hence, its representation flexibility. In this work, surfaces defined by 4×4 control points are employed.

The surface resolution has an impact on the performance of computing Bézier surfaces. For our method, this is a very important consideration since the computation of Bézier surfaces

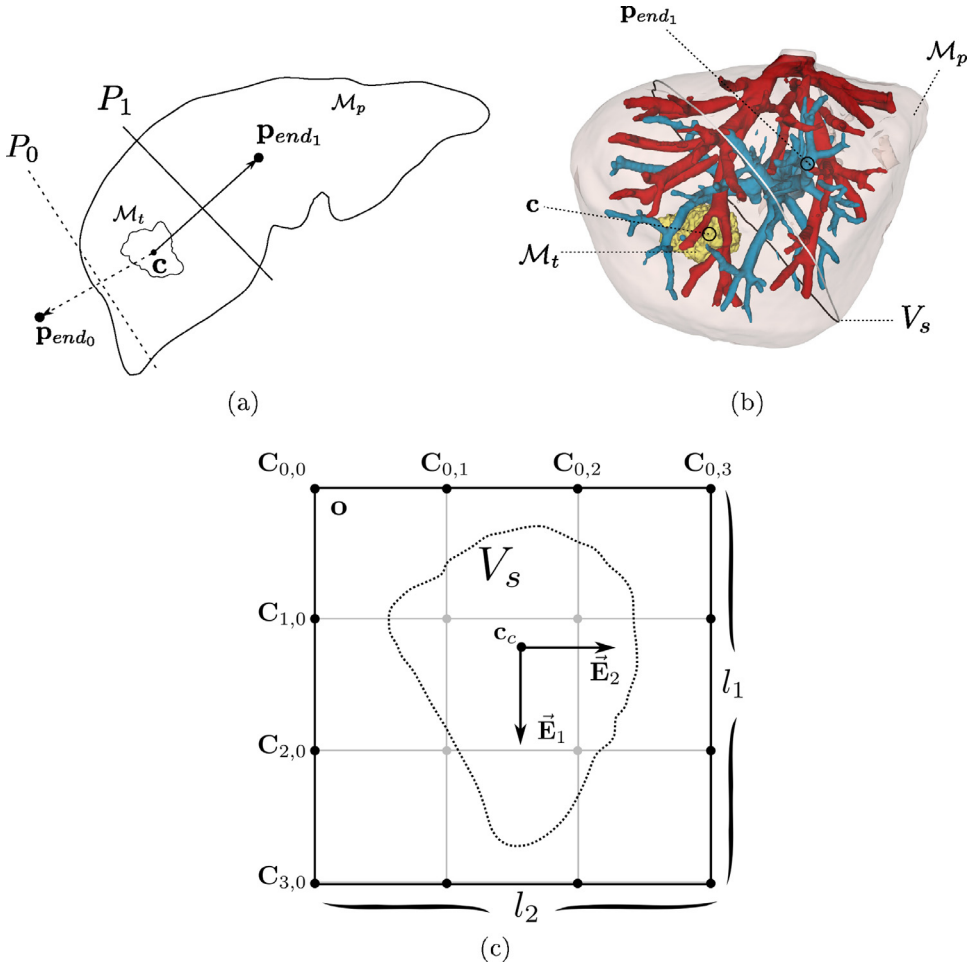

Fig. 2. Initialization of the resection: (a) 2D illustration of the initialization process where the initial point $\mathbf{p}_{end_0}$ (which produces the initial plane P_0), is moved to $\mathbf{p}_{end_1}$, thus producing the initial plane P_1; (b) 3D representation initial resection resulting at $\mathbf{p}_{end_1}$; (c) Geometry of the initial resection G based on PCA of the contour V_s.

Algorithm 2 Compute initial resection.

Precondition: Cross-section contour represented as the set of N 3D points $V_s = \{\mathbf{p}_i\}_{i=1}^{N}$. m and n determine the dimensions of the output control polygon.

function InitialResection(V_s, m, n)
  $\mathbf{c}_c \leftarrow Centroid(V_s)$ ▷ *Centroid of contour*
  $[e_1, e_2, \vec{\mathbf{E}}_1, \vec{\mathbf{E}}_2] \leftarrow PCA(V_s)$
  $l_1 \leftarrow 4\sqrt{e_1}$ ▷ *Width of resection plane*
  $l_2 \leftarrow 4\sqrt{e_2}$ ▷ *Height of resection plane*
  $\mathbf{o} \leftarrow \mathbf{c}_c - \frac{l_1}{2}\vec{\mathbf{E}}_1 - \frac{l_2}{2}\vec{\mathbf{E}}_2$ ▷ *Plane origin*
  for $i \leftarrow 1$ to m **do**
    for $j \leftarrow 1$ to n **do**
      $\mathbf{C}_{i,j} \leftarrow \mathbf{o} + \frac{il_1}{m}\vec{\mathbf{E}}_1 + \frac{jl_2}{n}\vec{\mathbf{E}}_2$
    end for
  end for
  $C \leftarrow \{\mathbf{C}_{i,j}\}_{i,j=1}^{m,n}$ ▷ *Control polygon*
  return C
end function

is followed by other processing stages (Section 3.4) and all the computations involved must be performed in real-time. In this work, surfaces of resolution 40 × 40 points are used.

Updating the resection surface when a control point changes its position requires re-computing the whole extent of the surface—the reader should notice that this is an inherent property of the formulation (Eq. (1). Algorithm 3 describes this process for surfaces of variable number of control points and resolution.

Algorithm 3 Update Bézier Surface.

Precondition: $\mathbf{C}$ being the grid of control points of size $m \times n$, and $r_u \times r_v$ representing the resolution of the surface.

function UpdateBezier($m, n, r_u, r_v, \mathbf{C}$)
  for $i \leftarrow 1$ to r_u **do**
    $u \leftarrow i/(r_u - 1)$
    for $j \leftarrow 1$ to r_v **do**
      $v \leftarrow j/(r_v - 1)$
      for $k \leftarrow 1$ to m **do**
        $B_u \leftarrow \binom{m}{k} u^k (1-u)^{m-k}$
        for $l \leftarrow 1$ to n **do**
          $B_v \leftarrow \binom{n}{l} v^l (1-v)^{n-l}$
          $\mathbf{S_{i,j}} \leftarrow \mathbf{C}_{i,j} B_u B_v$
        end for
      end for
    end for
  end for
  return S
end function

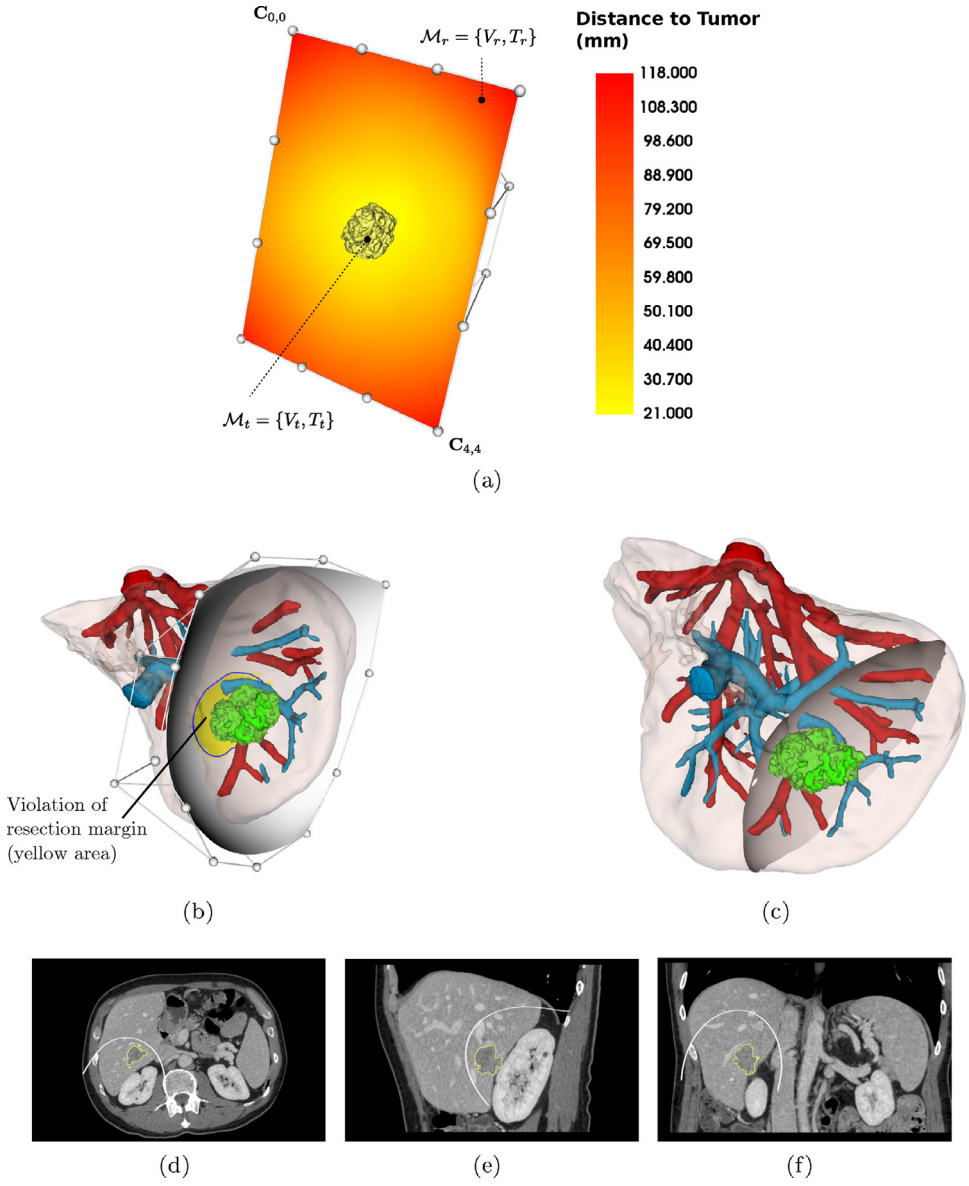

Fig. 3. Visualization of the resection path: (a) distance map derived from the tumor model $\mathcal{M}_t$ and the resection surface $\mathcal{M}_r$. (b) visualization of the resection surface given by a 3D Bézier surface and thresholding of the distance map using the resection margin; the violation of resection margin is highlighted in yellow (blue contour around); (c) visualization of the final resection surface where the control points and the resection exceeding the parenchyma are hidden; (d,e,f) projection of the resection surface into individual 2D slices with axial, coronal, sagittal orientation respectively.

3.4. 3D Visualization and projection in 2D slices

Together with the visualization of the 3D surface defining the virtual resection, our approach includes the visualization of the resection margin—which refers to the safety distance that should be kept between the resection surface and the tumors. The resection margin is updated when the resection is modified. In order to compute the resection margin, we employ the *point-to-surface* distance δ:

$$\delta(\mathbf{p}) = \min_{\forall \mathbf{q}_i \in V_t} \|\mathbf{p} - \mathbf{q}_i\| \ , \tag{9}$$

where V_t is the set of points of the tumor model $\mathcal{M}_t$ and $\mathbf{p}$ is a point belonging to the resection surface model $\mathcal{M}_r$; $\|.\|$ refers to the euclidean norm. The *point-to-surface* distance is computed for all points of the resection surface which effectively generates a distance map projected onto the resection surface (Fig. 3b). Using these distance maps, it is possible to determine the validity of the resection surface in terms of resection margin; for instance, if the margin set by clinicians is under 10 *mm*, then the resection would be valid only if all the points in the surface are further than 10 *mm* from the tumor.

For visualization purposes, we avoid the use of a color-map projected onto the surface. Visually, the color-map contains more information than clinicians need and all this information can be distracting. Instead, we threshold the distance map according to the resection margin. The areas violating the resection margin are then highlighted in yellow (with blue contour) while the rest of the surface remains in gray (Fig. 3b, 3c). The part of the Bézier surface exceeding the liver surface can be hidden as well as the net of control points (Fig. 3c). This facilitates the visualization of the resection by avoiding occlusions and simplifying the scene.

The projection of the surface onto individual 2D slices (Fig. 3d, 3e, 3f) is obtained by the intersection of axial, coronal and sagittal planes with the 3D Bézier surface.

3.5. Computation of resected volume

Computation of resection volumetry is a key functionality provided by existing software solutions for planning liver resections. Our approach to compute the resected volume consists of three steps. First, a high-resolution Bézier surface ($r_u = 300, r_v = 300$) is generated. Secondly, all the points of this high-resolution surface are mapped into a segmented image $M : \mathbb{R}^3 \rightarrow \{l_b = 0, l_p = 1, l_t = 2, l_r = 3\}$ (same dimensions and spacing as the original image taken from the patient for diagnosis), where the background (l_b), liver parenchyma (l_p), target tumors (l_t) and resection surface (l_r) are separated by different label values. The mapping of the high-resolution surface is performed on a basis of a $3 \times 3 \times 3$ voxels per surface point, which effect is the extrusion (thickening) of the mapped resection surface. This, together with the high-resolution construction of the surface, guarantees both continuity of the mapped surface and a clear boundary between the resected and the remnant volumes of the liver. Finally, a connected threshold region growing is applied (low threshold $l = l_p$ and upper threshold $u = l_r$) with a seed point arbitrarily chosen from a target tumor.

In order to compute volumes using this process, the resection path must enter and leave the parenchyma completely. This not only makes sense under the point of view of the application, but also guarantees a separation between the resected and the remnant volume.

3.6. User interaction

In order to keep the simplicity of use and flexibility of resection representation, we introduce two new interaction mechanisms: global translation of the resection surface and modification of control points in groups. An example of the possible sequence of interactions using these mechanisms, and leading to a valid resection plan is illustrated in Fig. 4.

Global translation of Bézier surfaces defined by a grid of 4×4 control points requires the modification of all the 16 control points—which implies a considerable number of user interactions. To avoid this, we set the control polygon connecting the control points as an interactive frame that can be moved through *drag-and-drop* interactions. Moving the frame produces a translation transformation on all control points which effectively produces the translation of the surface (Lemma 1.b).

Resections, regardless of their type, can be defined by a virtual resection resulting from a resection surface with *pseudo-parabolic* shape. For a resection surface defined by a grid of 4×4 control points, this implies the movement of either the 4 inner points of the grid or the 12 remaining (outer) points. In our implementation, simple mouse *right-click* on any of the 4 inner points will produce translation of all these points together. The same applies for the 12 outer points. This type of interaction allows the simple construction of *pseudo-parabolic* shapes, which can then be refined by individual modification of the control points. For illustration purposes we refer to Fig. 2c, where the 4 inner points are shown in light-gray, while the 12 outer are shown in black.

4. Evaluation methodology

In order to validate and evaluate the proposed method we perform a user study which includes a comparison with our own implementation of CP and DS in 3D Slicer [16]. The implementation details of CP and DS are described in the following and summarized in Table 1.

The implementation of the CP approach is based on [13] and [15]. This approach uses a surface with a variable mesh resolution $30 \times n$ square quads, where 30 is the number of quads in the short axis and n is the number of square quads needed to fill the extent of the plane (Eq. (6)) in the long axis.

Implementation of DS is based on the general principles established in [13] combined with design aspects in [14]. In this implementation, the user can draw and overwrite complete traces individually over the set of 2D slices. Navigation between traces was implemented so the user could easily find individual traces and their corresponding slices. Parametric linear interpolation was applied to individual traces to obtain a regularly spaced sampled traces (20 points per trace). The final surface was computed by means of parametric quadratic interpolation between the traces, which requires at least 3 traces. Modification of the surface was allowed on the basis of traces, this is, redrawing of one or more traces and fast re-computation of the interpolated surface.

Study design and quantitative analysis are performed according to [22], which provides a comprehensive guide for the design and data analysis of experiments similar to the one presented in this work. In order to compare the different methods we establish the criteria and their corresponding objective evaluation metrics described in the following.

Preservation of resection margin. This criteria is concerned with how accurately the resection margin is preserved. This is measured by means of the minimum *point-to-surface* distance between the tumor and the resection surface derived from Eq. (9).

Inter-subject reproducibility of results. Surgery planning tools are essentially geometric modeling methods. This criteria considers how accurately different users can reach the same resection plan. In order to measure similarity of resections between users, we measure the resection volume difference (in %) with respect to the reference resection volume. Volumetry of resection is computed using the procedure in Section 3.6.

Planning time. Integration in the clinical work-flow is of paramount importance for new computational methods. Therefore the planning time should improve, or at least be similar, with respect to *state-of-the-art* methods.

Smoothness of results. Resection smoothness is a desirable feature. Smoothness not only helps the interpretation and visualization of 3D models, but also increases the feasibility of performing the planned resection during surgery (e.g., *"curvy"* surfaces are more difficult to perform surgically and sometimes even impossible). As indicator of surface smoothness we use the mean curvature [23]:

$$H = \frac{\mathcal{K}_1 + \mathcal{K}_2}{2} \tag{10}$$

where $\mathcal{K}_1$ and $\mathcal{K}_2$ are the principal curvatures.

4.1. Study design

Our approach to evaluate and compare the three different planning methodologies (in the following: Bézier, CP and DS) is the design of a study where the three planning techniques are used by the same expert users in different clinical cases. The group of participants consists of 5 gastro-intestinal surgeons ({5,8,10,11,31} years of clinical experience).

The evaluation was conducted using a data-set consisting of 5 patient-specific models (obtained from the Oslo-CoMet study [24]). This data-set includes CT volumes, segmentation and 3D modeling of vessels, parenchyma (liver surface) and tumors. From this data-set, each surgeon generated 8 virtual resections (all atypical resections). Some of these resections target either single or multiple tumors. For comparison purposes and in order to avoid differences in clinical criteria—which could potentially lead

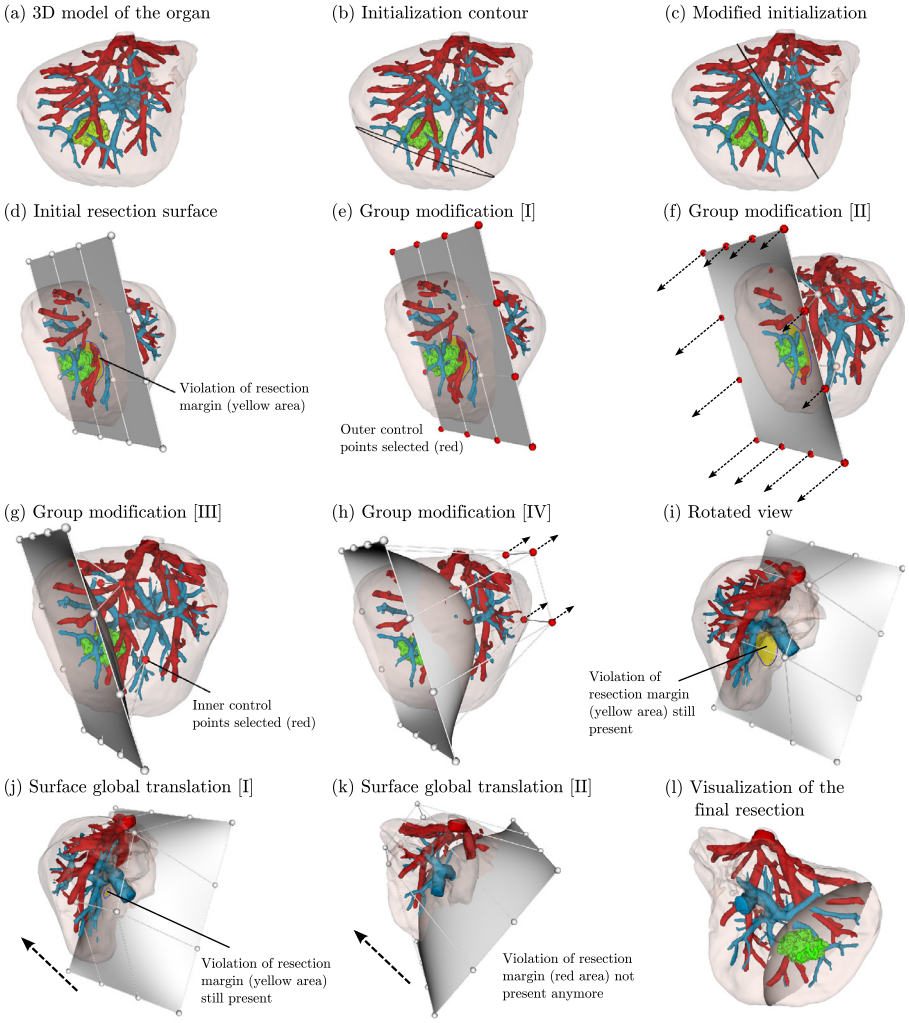

Fig. 4. Instance of liver resection planning using the proposed method including the proposed user interaction techniques. The sequence of interactions (a) to (d) illustrates the process of obtaining the initial approximation of the resection surface. (e) and (f) show the modification of the group of outer control points. In a similar way, (g) and (h) show the modification of the inner group of control points. In (i) a rotation of the view is performed. Later, in (j) and (k) the surface is translated (globally). Finally in (l) the visualization of the final resection is presented. The reader should notice, that from (d) to (j) the resection presents a yellow (blue contour around) area indicating the violation of the resection margin (arbitrarily set at 20*mm*). In (k) the resection margin is preserved (no yellow area in the surface) indicating validity of resection in terms of safety margin.

Table 1
Implementation aspects for DS, CP and Bézier.

Aspect	DS	CP	Bézier
Underlying representation	Bi-quadratic polynomial	Discrete grid	Bi-cubic polynomial
Surface resolution	20×20	$30 \times n$	40×40
Visualization	2D Slices / 3D Models	3D Models	3D Models
Resection margin visualization	✗	✗	✓
Interaction	1. Drawing in slices (3–5) traces	1. Traces on parenchyma 2. Local deformation	1. Slicing plane on parenchyma 2. Bézier deformation

to different resection plans for the same tumors—a set of resection plans was employed as reference. The reference set (median resected volume 208.98 *ml*) was generated by the most experienced surgeon in an earlier pilot study (3 months earlier). All the participants were asked to perform the same resection plan as in the reference. To do this, the participants were allowed to explore ($<$ 5 minutes) the reference resection plan beforehand. The experts' comments were recorded after each resection plan (see Section 5).

4.2. Procedure

Before starting the experiments (during the same session), the surgeons were shown the graphical user interface and the process to obtain resections with the different methods (CP, DS, Bézier). Surgeons were allowed to use the system to perform a sample resection as training ($<$ 1 *h*).

The experiment consisted of planning the different cases using CP, DS and Bézier for all the cases. The cases were ordered for all the participants, however, the order of the method is *a-priori* randomized to reduce the impact of confounding factors (i.e., training or sequence effects). The participants were allowed get help by a technician on any technical aspect related to the use of the interface whenever needed (due to the short training session). A resection plan was considered finalized when the participant indicated (either by obtaining the desired resection or believing the plan cannot be further improved) and the verification by a technician

Table 2
Descriptive analysis derived from the quantitative evaluation.

Method		Time (s)	Deviation from Margin (mm)	Deviation from Volume (%)	Median Mean Curv. (1/m)
Bézier	min	53.00	−3.25	−10.15	0.00
	25%	126.50	0.13	−1.83	0.01
	50%	174.00	0.42	−0.40	0.01
	75%	244.00	1.47	1.17	0.02
	max	801.00	6.05	3.77	0.02
CP	min	42.00	−9.84	−8.97	0.01
	25%	129.75	−7.65	−4.93	0.03
	50%	180.50	−4.75	−2.40	0.03
	75%	250.50	−1.04	−0.56	0.04
	max	748.00	5.46	3.21	0.11
DS	min	44.00	−7.98	−7.07	0.01
	25%	116.75	−3.51	−3.31	0.01
	50%	179.00	−1.49	−1.39	0.02
	75%	345.00	0.12	0.32	0.02
	max	757.00	8.53	6.69	0.04

Table 3
Comments from the experts (S1-S5 indicates the participant who provided/expressed the comment).

General comments
[**GC1**] Undo functionality would be useful (S1, S4).
[**GC2**] Ability to set transparency of surfaces would be useful (S1, S5)
[**GC3**] Pre-defined views aligned to surgical way of looking at the liver would be useful (S1).
[**GC4**] Rotation of resection can be useful in some cases, specially in CP and Bézier (S1).
Comments on DS
[**CDS1**] Poses the steepest learning curve / is the least intuitive method (S1, S2, S3, S5).
[**CDS2**] Can be difficult to specify resections with high curvature (S1, S5).
[**CDS3**] Can be adequate for *quasi-planar* resections (S1).
[**CDS4**] Could not reach exactly the desired resection in some cases (S2, S3).
[**CDS5**] Some resections could be better defined by combination of traces in different views (axial, coronal, sagittal) (S3).
Comments on CP
[**CCP1**] Resections derived from drawing traces in parenchyma sometimes produce unexpected results in terms of desired curvature (S1, S3).
[**CCP2**] Modification of resections in CP present more degree of freedom (complexity) than needed. More simplicity would be a benefit (S1,S3).
[**CCP3**] *"Curvy/Bumpy/Wavy"* resection plans derived from CP can be difficult to perform surgically (S1, S3, S4, S5).
[**CCP4**] Local deformations can be useful in particular cases like peripheral metastases (S3 ,S5).
[**CCP5**] Deformation can be difficult when the initial plane is nearly perpendicular to the screen plane (S4).
Comments on Bézier
[**CB1**] Visualization of resection margin is an advantage of this method (S1).
[**CB3**] In addition to visualization of the margin on the surface, a global warning of resection violation could be useful. Sometimes violation or resection is occluded (S2).
[**CB4**] Deformation of resection in Bézier does not look obvious (S4).
[**CB5**] Bézier is the most intuitive method (S5).

that the resection was complete (surface exceeds the parenchyma in all directions). Time to complete the resection plan (excluding technician assistance in questions related to user interaction and verification of resection) was recorded, together with the geometry of the 3D surface models derived from the resection plan.

5. Results

In this section, we present results derived from the use CP, DS and Bézier by clinicians at Oslo University Hospital, as described in Section 4. A descriptive analysis of quantitative results is shown in Table 2. Subjective feedback of the participants—which will be use as a base for discussion in Section 6—is recorded in Table 3.

In the same line as [22], we conduct statistical tests for normality of data (*Shapiro-Wilk*), difference between methods (*ANOVA, Friedman*) and pairwise differences between methods (*Wilcoxon, paired Student's t-test*) with *Bonferroni* correction [25]. Due to the Bonferroni correction, all effects derived from pairwise comparisons are reported at a 0.0167 (i.e., one third of the p-value 0.05) level of significance. Statistical analysis was carried out with the R statistics software package.

Surgery Planning Time. The surgery planning time was recorded for every resection performed by the participants (Fig. 5a). The Friedman test reveals no significant difference between methods in terms of time, with $\chi^2(2) = 1.849,\ p = 0.39 > 0.05$, where the median completion times were $174\,s$ for Bézier, $179\,s$ for DS and $180\,s$ for CP.

Deviation from Resection Margin. Pairwise comparison between methods in terms of deviation from resection margin (Fig. 5b) through Wilcoxon signed-rank test yields:

- $V = 164,\ p = 0.0006 < 0.167$ between CP and DS,
- $V = 32,\ p = 5.03e-09 < 0.167$ between CP and Bézier,
- $V = 75,\ p = 8.69e-07 < 0.167$ between DS and Bézier.

These results show significant differences regarding the deviation of resection margin between methods. The median deviations from resection margin were $0.42\,mm$ for Bézier, $-1.49\ mm$ for CP and $-4.74\ mm$ for DS. Bézier presents the least deviation from resection margin. The number of resections violating the resection margin ($dev < -0.01$) is $v_{cp} = 31$ for CP, $v_{ds} = 28$ for DS and $v_{bez} = 1$ for Bézier.

Deviation from Reference Volume. Deviation from the reference volume (Fig. 5c was computed as the difference (in %) between the resected volumes obtained by the participants and their cor-

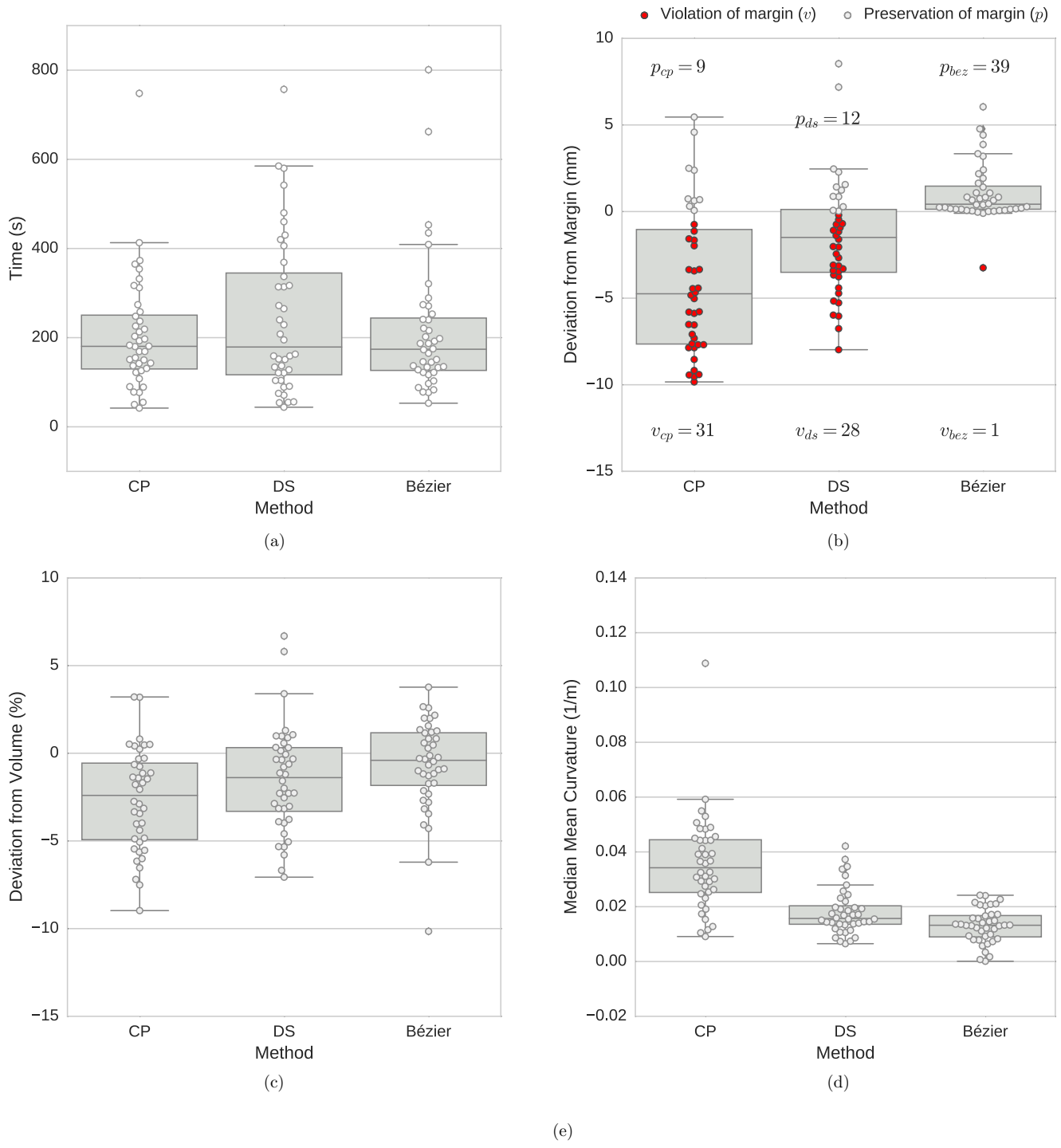

Fig. 5. Box plots of results derived from the quantitative evaluation: (a) time, (b) deviation from margin which includes the number of resections violating the margin ($dev < -0.01\ mm$ marked in red) and the number of resections preserving the margin ($dev \geq -0.01\ mm$), (c) deviation from volume and (d) median mean curvature.

responding resected volumes in the reference data-set. Wilcoxon signed-rank test yields:

- $V = 308,\ p = 0.174 > 0.0167$ between CP and DS,
- $V = 67,\ p = 3.875e-07 < 0.0167$ between CP and Bézier,
- $V = 190,\ p = 0.0025 < 0.0167$ between DS and Bézier.

Pairwise tests show significant differences between Bézier and the other two methods. The median volume deviation is −0.4% for Bézier, −1.39% for DS and −2.40% for CP. Bézier shows the least deviation with respect to the reference resected volume.

Resection Curvature. Pairwise comparison of resection curvature between methods (Fig. 5d) through Wilcoxon signed-rank test yields:

- $V = 638,\ p = 0.001 < 0.167$ between CP and DS,
- $V = 654,\ p = 0.007 < 0.167$ between CP and Bézier,
- $V = 475,\ p = 0.39 > 0.167$ between DS and Bézier.

These results show that the difference in curvature for CP is different from both DS and Bézier. No significant difference was found between Bézier and DS. Median mean curvature is 0.01 m^{-1}

for both Bézier and DS, and 0.03 m^{-1} for CP. Both Bézier and DS produce resections with lower curvature than CP.

6. Discussion

Computer-assisted systems for planning and guiding liver resections have existed for nearly two decades now. Although some of these systems have made their way into clinical reality, none of them seem to be established as a *gold-standard* solution replacing previous clinical practices. To a great extent, this is due to the difficulties of generating the patient-specific models employed by these systems—segmentation, for instance, is still considered a research problem and a bottleneck for the generation of patient-specific models. No consensus exists about planning liver resections—DS and CP approaches currently coexist in the surgery planning market. New methods for planning liver resections should, at least, highlight their differences, as well as their advantages/disadvantages with respect to the existing techniques. Therefore, in this section, a comparison of our approach with DS and CP strategies is discussed on the basis of the results presented in Section 5.

According to our results, the required time (median) for completion of a resection plan using the proposed method ($t = 174\ s$) is, as low as for the *state-of-the-art* methods CP ($t = 180\ s$) and DS ($t = 179\ s$). This indicates that the adoption of the proposed method in the clinical routine would not imply any significant change in the clinical work-flow.

Bézier shows the least deviation from the reference plan in terms of volume (−0.40%) compared to DS (−1.39%) and CP (−2.40%). In our study, small deviations from resected plans are expected from all the methods since the median resected volume for the reference data-sets is relatively small (208.98 ml); larger deviations in volume are expected for larger resections (e.g., hemihepatectomies).

The comments from the participants show wide consensus on considering DS the most difficult method to use (**CDS1**), particularly for resections exhibiting higher curvature (**CDS2, CDS3**). Furthermore, in some cases, DS did not provide satisfactory results (**CDS4**); to mitigate these problems, the ability to combine traces in different views is suggested (**CDS5**). No consensus was found on whether CP or Bézier is the most intuitive (**CCP2, CB4, CB5**). Considering task completion time as indicator of usability, and despite the fact that no statistical significance between the methods was found, the higher variability of DS with respect to CP and Bézier seems to support that DS is less intuitive than CP and Bézier, which are comparable in this regard.

As discussed in [15], continuous visualization of distance from the resection surface to the tumor is a desirable feature since it is associated with the preservation of resection margin. Our results show the visualization technique proposed in Section 3.4 is an effective mechanism (**CB1**) to avoid violations of resection margin ($v_{bez} = 1$ for Bézier compared to $v_{cp} = 31$ and $v_{ds} = 28$); median deviation from resection margin is also lower using Bézier (0.42 mm) as compared to using CP (−4.75 mm) or DS (−1.49 mm). Despite the good results in terms of preservation of resection margin of our proposed method, this was not sufficient to avoid all the violations of resection margin; occlusions of resection margin visualization (e.g., by vessels) might lead to unnoticed resection violations. To avoid this, and in line with the participants' comments (**CB3**), an indicator of margin violation external to the visualization of the surface should be provided (e.g., bi-color state widget in the GUI or a warning icon).

The shape of the virtual resection is an important aspect since it relates to the feasibility of performing the resection surgically; resections presenting *wavy* resection trajectories might be not realizable during surgery as they are specified in the virtual plan. In this sense, resections presenting low curvature are associated with higher surgical feasibility than resections with high curvature. According to our results, Bézier and DS provide resections which are easier to perform surgically (lower curvature) compared to CP. In this line, and according to the participants' comments (**CCP3**), using CP might lead to resections that are difficult to perform surgically.

Some of the techniques described in this work can be employed to improve CP and DS; visualization of resection margin (**CB1**), for instance, was already discussed in [15] as a possible improvement. Some other improvements suggested in our experiments by the experts users, like the possibility of a semi-transparent visualization of resection surface (**CG2**) and the possibility to undo actions (**CG1**) were also found in [15] and should be considered for further improvement of all the methods. Rotation of the resection, particularly for CP and Bézier (**GC4**), and predefined alignments of the 3D view to surgical positions (e.g., anterior-posterior axis) (**GC3**) could be implemented for methods other than Bézier.

Despite that our method showed good performance in terms of planning time, reproducibility of results, preservation of margin and curvature, expert users highlight scenarios where the use of DS and CP could be still advantageous—such as for *quasi-planar* resections (**CDS3**) like hemihepatectomies or small local resections like peripheral metastases (**CCP4**). In this regard, and since all the methods are similar in terms of time, software platforms for planning liver resections could consider including all the methods to provide clinicians with greater flexibility to represent resections. Furthermore, CP and Bézier could even be combined so that local deformations like in CP are preceded by global deformations like in Bézier.

7. Conclusion

In this work we propose a novel method for planning liver resection procedures. This method is based on the use of deformable Bézier surfaces for the specification of resection geometry and the projection of risk areas (representing violations of safety margins) onto the resection surface through distance maps. Our implementation of the method includes mechanisms to reduce the number of interactions making the system easy-to-use by clinicians.

Our experimental results show that the planning time of our method is as low as *state-of-the-art* methods, and therefore, can be integrated in the clinical reality without modifications in the clinical work-flow. Our method, not only shows superior preservation of resection margin methods, but also higher reproducibility of surgery planning results than *state-of-the-art*. In addition, the proposed method provides smooth virtual resections presenting high feasibility to be performed surgically (e.g., absence of sharp corners and wavy trajectories).

Acknowledgments

This work was supported by the Research Council of Norway through the Hypercept project (number 221073), and The Intervention Centre, Oslo University Hospital (Norway). Authors thank Leonid Barkhatov, David Aghayan, Sheraz Yaqub, Mushegh Sahakyan, Kristoffer Lassen and Bård I. Røsok for fruitful discussions and their contribution to the evaluation of the method proposed in this work. Authors would like to thank also Xiaoran Lai for reviewing the data analysis.

References

[1] L.A. Torre, F. Bray, R.L. Siegel, J. Ferlay, J. Lortet-tieulent, A. Jemal, Global cancer statistics, 2012, CA: A Cancer J. Clin. 65 (2) (2015) 87–108, doi:10.3322/caac.21262.

[2] C. Couinaud, Le foie: études anatomiques et chirurgicales, Masson & Cie, 1957.

[3] R.J. Aragon, N.L. Solomon, Techniques of hepatic resection, J. Gastrointest. Oncol. 3 (1) (2012) 28–40, doi:10.3978/j.issn.2078-6891.2012.006.
[4] E. Vanni, E. Bugianesi, Obesity and liver cancer, Clin. Liver Dis. 18 (1) (2014) 191–203, doi:10.1016/j.cld.2013.09.001.
[5] R. Bryant, A. Laurent, C. Tayar, J.T. van Nhieu, A. Luciani, D. Cherqui, Liver resection for hepatocellular carcinoma, Surg. Oncol. Clin. N. Am. 17 (3) (2008). 607–33, ix doi: 10.1016/j.soc.2008.02.002.
[6] E.P. Misiakos, N.P. Karidis, G. Kouraklis, Current treatment for colorectal liver metastases., World J. Gastroenterol. : WJG 17 (36) (2011). 4067–75 doi: 10.3748/wjg.v17.i36.4067.
[7] M.J. Schuchert, B.L. Pettiford, J.D. Luketich, R.J. Landreneau, Parenchymal-sparing resections: why, when, and how, Thorac. Surg. Clin. 18 (1) (2008) 93–105, doi:10.1016/j.thorsurg.2007.11.007.
[8] G. Vennarecci, A. Laurenzi, R. Santoro, M. Colasanti, P. Lepiane, G.M. Ettorre, The ALPPS procedure: a surgical option for hepatocellular carcinoma with major vascular invasion, World J. Surg. 38 (6) (2014) 1498–1503, doi:10.1007/s00268-013-2296-y.
[9] W. Lamadé, G. Glombitza, L. Fischer, P. Chiu, C.E. Cárdenas, M. Thorn, H.P. Meinzer, L. Grenacher, H. Bauer, T. Lehnert, C. Herfarth, The impact of 3-dimensional reconstructions on operation planning in liver surgery., Arch. Surg. (Chicago, Ill. : 1960) 135 (11) (2000). 1256–61
[10] H. Lang, A. Radtke, M. Hindennach, T. Schroeder, N.R. Frühauf, M. Malagó, H. Bourquain, H.-O. Peitgen, K.J. Oldhafer, C.E. Broelsch, Impact of virtual tumor resection and computer-assisted risk analysis on operation planning and intraoperative strategy in major hepatic resection., Arch. Surg. (Chicago, Ill. : 1960) 140 (7) (2005). 629–38; discussion 638 doi: 10.1001/archsurg.140.7.629.
[11] C. Hansen, S. Zidowitz, B. Preim, Impact of model-based risk analysis for liver surgery planning, Int. J. Comput. Assist. Radiol. Surg. 9 (3) (2014). 473–80 doi: 10.1007/s11548-013-0937-0.
[12] P. Lamata, F. Lamata, V. Sojar, P. Makowski, L. Massoptier, S. Casciaro, W. Ali, T. Stüdeli, J. Declerck, O.J. Elle, B. Edwin, Use of the resection map system as guidance during hepatectomy., Surg. Endosc. 24 (9) (2010). 2327–37 doi: 10.1007/s00464-010-0915-3.
[13] B. Preim, C.P. Botha, Visual computing for medicine: theory, algorithms, and applications, 2nd, Newnes, 2013.
[14] L. Ruskó, I. Mátéka, A. Kriston, Virtual volume resection using multi-resolution triangular representation of B-spline surfaces., Comput. Methods Programs Biomed. 111 (2) (2013). 315–29 doi: 10.1016/j.cmpb.2013.04.017.
[15] O. Konrad-Verse, A. Littmann, B. Preim, Virtual resection with a deformable cutting plane., in: SimVis, 2004, pp. 203–214.
[16] 3D Slicer, http://www.slicer.org/.
[17] L. Piegl, W. Tiller, The NURBS Book (2nd Ed.), Springer-Verlag New York, Inc., New York, NY, USA, 1997.
[18] J. Gallier, Curves and Surfaces in Geometric Modeling: Theory and Algorithms, Morgan Kaufmann Publishers Inc., San Francisco, CA, USA, 2000.
[19] G. Morin, R. Goldman, On the smooth convergence of subdivision and degree elevation for bézier curves, Comput. Aided Geom. Des. 18 (7) (2001) 657–666, doi:10.1016/S0167-8396(01)00059-0.
[20] W. Lorensen, H. Cline, Marching cubes: a high resolution 3D surface construction algorithm, ACM Siggraph Comput. Graphics 21 (4) (1987) 163–169.
[21] T.S. Newman, H. Yi, A survey of the marching cubes algorithm, Comput. Graphics 30 (5) (2006) 854–879, doi:10.1016/j.cag.2006.07.021.
[22] S. Glaßer, P. Saalfeld, P. Berg, N. Merten, B. Preim, How to evaluate medical visualizations on the example of 3D aneurysm surfaces, Eurographics Visual Computing for Biology and Medicine, August, 2016, doi:10.2312/vcbm.20161283.
[23] R. Goldman, Curvature formulas for implicit curves and surfaces, Comput. Aided Geom. Des. 22 (7 SPEC. ISS.) (2005) 632–658, doi:10.1016/j.cagd.2005.06.005.
[24] A.A. Fretland, A.M. Kazaryan, B.A. Bjornbeth, K. Flatmark, M.H. Andersen, T.I. Tonnessen, G.M.W. Bjornelv, M.W. Fagerland, R. Kristiansen, K. Oyri, B. Edwin, Open versus laparoscopic liver resection for colorectal liver metastases (the Oslo-CoMet study): study protocol for a randomized controlled trial, Trials 16 (1) (2015) 1–10, doi:10.1186/s13063-015-0577-5.
[25] J.P. Shaffer, Multiple hypothesis testing, Annu. Rev. Psychol. 46 (1995) 561–584, doi:10.1016/S1573-4412(84)02006-7.